This article has been accepted for publication in a future issue of this journal, but has not been fully edited. Content may change prior to final publication. Citation information: DOI 10.1109/JQE.2016.2643279, IEEE Journal of Quantum Electronics

A Broadband Terahertz Metamaterial Absorber Based on Two Circular Split Rings

Wu Pan, Xuan Yu, Jun Zhang, Wei Zeng

***Abstract*—We present a broadband terahertz metamaterial absorber, of which the unit cell is made up of two cirular split rings, a dielectric substrate and a metallic ground. The simulation results show that the absorber achieves a broadband absorption from 0.85THz to 1.926THz with the absorptivity beyond 90% at normal incidence, and the bandwidth is 1.076THz which is 77.52% with respect to the central frequency. The broadband and high absorption is mainly resulted from the strong electromagnetic resonance and overlapping of resonant frequencies. Moreover, the proposed absorber has a property of wide angle absorptivity for both TE and TM polarizations, and thus can play an important role in terahertz imaging, detecting and stealthy technology.**

***Index Terms*—terahertz; metamaterial; broadband absorption; split ring**

I. Introduction

In recent years, metamaterials have attracted increasing attentions due to their exotic electromagnetic properties that are unavailable in nature, such as negative refractive index[1], invisibility[2], perfect lensing[3], and perfect absorbing[4]. Because of those novel properties, many devices[5-7] based on metamaterials have been demonstrated. One burgeoning branch of the practical devices is metamaterial absorber, which can achieve a nearly perfect absorption at the resonance frequencies. The first perfect metamaterial absorber was demonstrated by Landy et al[8] in 2008.The absorber with a classic sandwiched structure composed of a split ring resonator, a dielectric substrate, and a metallic cut wire achieved its peak absorption of 88% at 11.5GHz. Since then, a great number of metamaterial absorbers have been proposed in different frequency ranges including microwaves[9-10], terahertz[11-12], visible and infrared bands[13-14]. Due to the remarkable advantages of near unity absorption, ultra-thin thickness and tunability, metamaterial absorbers have many potential applications in micro-bolometer, spectral imaging, photodetector and solar cells. However, most of the reported absorbers have common drawbacks of single working frequency and narrow absorption bandwidth, which greatly limits their practical applications. In order to solve the problem, dual-band[15-17], multi-band[18-20] and broadband[21-22] absorbers were demonstrated in the past few years. Especially in the cases such as broadband sensor and modulator, micro-bolometer, broadband antireflection coatings, absorbers with broadband width are required. Generally, there are two major methods to expand the absorption bandwidth: one effective method is vertically stacking multiple metal-dielectric layers[23-25], another approach is to form a coplanar structure consisted of multiple resonators of different sizes[4,26]. However, with the increasing of metal-dielectric layers, the first method requires strict processing, and the fabrication may become inconvenient and time-consuming. The second method has the disadvantages of large unit size and limited working frequency. So, when pursuing the large absorption bandwidth, many researchers also devote to designing simpler structures. Recently, Bhattacharyya et al[27-28] presented a simple structured metamaterial absorber which achieves an octave bandwidth in the microwave range. Their studies show great significance in the structure design of metamaterial absorber.

In this paper, different from the two methods mentioned above, we present a simple structured metamaterial absorber of three layers composed of double circular split rings and a grounded metallic film separated by a dielectric substrate. The simulation results exhibit a broadband absorption from 0.85THz to 1.926THz with the absorptivity beyond 90% at normal incidence, and the bandwidth is 1.076THz which is 77.52% with respect to the central frequency. The high absorptivity can also be achieved at wide incidence angles for both TE and TM waves. To illustrate the absorption mechanism, the surface current distributions, energy density of electric field and energy density of magnetic field are introduced. Furthermore, the concept of the presented absorber can also be applied to a double square split rings structure and can be scaled up to work at microwave frequency regimes. Thus, the idea of the presented absorber provides us more flexible structures and wider working frequencies.

II. Structure and Design

The current paper presented a perfect metamaterial broadband absorber working at terahertz regime. The structural schematic diagram of the absorber unit cell and the direction of incident wave are illustrated in Fig.1. The unit cell is a classic three layered structure composed of two double splits circular rings and a metallic continuous film separated by a dielectric substrate. The repeat period is $P=P_x=P_y=70\mu m$, the radii of circular rings are $r_1=30\mu m$, $r_2=27\mu m$, $r_3=16\mu m$, $r_4=13\mu m$, and the gap of the split ring $w=w_1=w_2$ is set to be 4μm. The presented absorber was simulated and optimized based on the commercial finite difference time domain (FDTD) solver CST Microwave Studio 2012, where we set unit cell boundary condition along

This article has been accepted for publication in a future issue of this journal, but has not been fully edited. Content may change prior to final publication. Citation information: DOI 10.1109/JQE.2016.2643279, IEEE Journal of Quantum Electronics

the lateral directions and open(add space) boundary condition along the z-direction. In our simulation, the double splits circular rings and metallic continuous film were made of lossy gold with a conductivity of σ =4.56×10^{7}S/m and a thickness of 0.4μm. The dielectric material was typical lossy polyimide with a dielectric constant of ε=3(1+i0.06)[29] and a thickness of 26μm. The absorptivity $A(\omega)$ can be obtained by[30] $A(\omega)$=1-$R(\omega)$-$T(\omega)$, where $R(\omega)$ represents the reflectivity, $T(\omega)$ represents the transmissivity. Because of the existence of bottom continuous metallic film, the transmissivity is zero, and the absorptivity can be expressed as $A(\omega)$=1- $R(\omega)$.

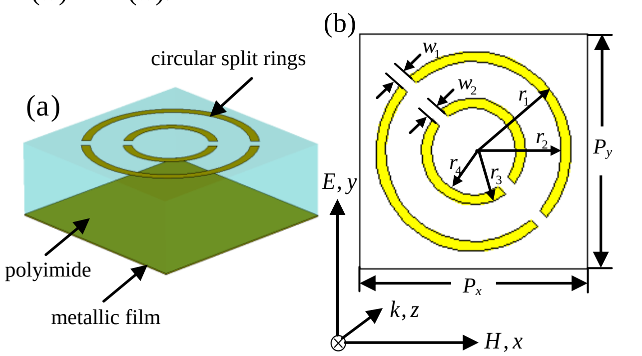

Fig. 1. Schematic diagram of the proposed metamaterial absorber unit cell

III. SIMULATION RESULTS AND DISCUSSION

The simulation results of the absorption curves are depicted in Fig.2. As shown in Fig.2, a broadband absorption from 0.85THz to 1.926THz with the absorptivity beyond 90% for both TE and TM waves is achieved. In Fig.2, TE and TM waves get exactly the same absorption curve, and it is mainly due to the symmetry of the absorber structure. Then we extract the effective permittivity, effective permeability and effective impedance of the current design via inversion of S parameters[31] as shown in Fig.3 and Table 1. In Fig.3(c), it can be observed that from 0.85THz to 1.926THz, the real part of the effective impedance is closely near unity(Re(z)≈1) which indicates matching to the free space, and the imaginary part is close to zero(Im(z) ≈0). The derived effective impedance shows a great agreement with the absorptivity. Table 1 shows the calculated data at the three peak absorptions. The real part of permeability is negative, which indicates a realization of magnetic metamaterial[32]. And from the equation $z=\sqrt{\mu/\varepsilon}$ [33], we find that the calculated effective impedance of the medium also matches well with the free space impedance at the three peak frequencies.

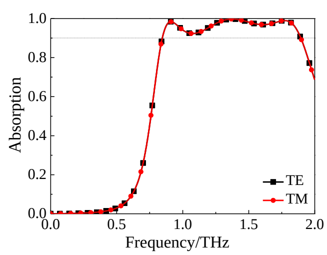

Fig.2. Simulated absorption spectra for both TE and TM waves.

In order to reveal the physical origin of the proposed broadband absorber, surface current distributions, energy density of electric field and magnetic field at the three peak absorptivity frequencies, which are 0.91THz, 1.374THz and 1.772THz, are depicted in Fig.4.

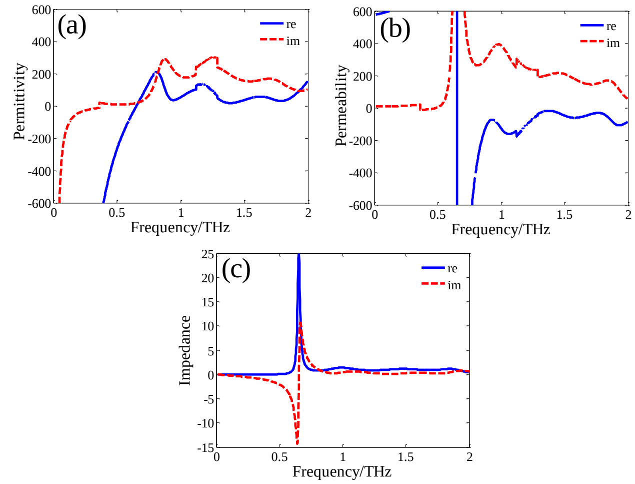

Fig.3. Calculated (a) real and imaginary part of the effective permeability (b) real and imaginary part of the effective permittivity (c)real and imaginary part of the effective impedance of the proposed absorber.

Table 1 The real and imaginary part of the effective permittivity, effective permeability and effective impedance at the frequencies of three peak absorptions

Frequency (THz)	ε_{eff}		μ_{eff}		z_{eff}	
	Re	Im	Re	Im	Re	Im
0.91	46.23	258.1	-77.11	347.20	1.15	0.23
1.374	18.30	198.1	-19.21	207.50	1.02	0.09
1.772	31.65	151.4	-32.21	154.20	0.99	0.21

It is clear that at 0.91THz and 1.374THz, the current flow and electromagnetic energy are mainly concentrated at the outer ring, and at 1.772THz, they concentrate at both the inner and outer rings. The three absorption peaks are corresponding to three resonant frequencies, respectively. The resonances can be equivalent to LC resonant circuits[34], as shown in Fig.4, the current flow starts from the area where the energy density of electric field is maximum, and it passes the area where the energy density of magnetic field is maximum. The energy of electric field is mainly concentrated at the splits which can be equivalent to capacitive elements that responsible for electric resonance, and the energy of magnetic field is mainly concentrated on the metallic line which can be equivalent to inductive elements that responsible for magnetic resonance. The energy distributions of the three peak resonances indicate strong electric and magnetic resonances in the absorber structure, and it mainly occurs at the top metallic layer. The energy is then converted into heat energy by the electromagnetic resonances. Thus, from the overlap of the three resonant frequencies, absorption of broadband width can be obtained. Furthermore, to get an insight of the loss mechanism, we simulate the absorption spectra under two different loss conditions (lossy and loss-free) of the dielectric layer. The results are depicted in Fig.5. As observed from the

This article has been accepted for publication in a future issue of this journal, but has not been fully edited. Content may change prior to final publication. Citation information: DOI 10.1109/JQE.2016.2643279, IEEE Journal of Quantum Electronics

absorption spectra, the three absorption peaks (resonant frequencies) are maintaining the same and so is the bandwidth with the absorptivity greater than 90%. Most importantly, from Fig.5, we can know that almost all the energy of the incident waves is dissipated in the top metallic layer (i.e. ohmic losses), which is very different from the previous study.[11,29]. And it makes the absorber less sensitive to the material of the dielectric layer and may have great potential applications in some areas where the metallic absorption is needed. The simulated results show an excellent agreement with the analysis above.

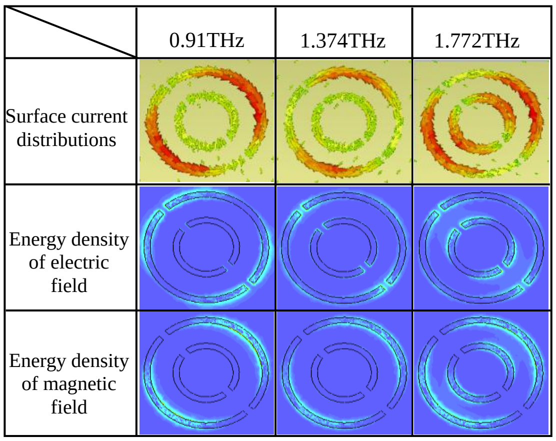

Fig.4. Surface current distributions, energy density of electric field and magnetic field of the metamaterial absorber.

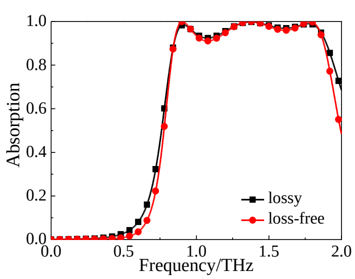

Fig.5. Dependence of the absorption spectra of the proposed absorber on two different loss conditions (lossy and loss-free)

We next investigate the influence of different incident angles on the absorption performance in Fig.6. As for TE wave in Fig.6(a), a broadband absorption can be maintained to 30° with the absorptivity nearly beyond 80%, with the increase of the incident angle, the absorptivity drops sharply, especially around 1.374THz. This is because when the incident angle increases, the magnetic component of the incident wave decreases and can no longer induce effective magnetic resonances. And at 1.374THz, the peak absorption is mainly due to the strong magnetic resonance, so with the magnetic flux decreasing, the peak absorption drops sharply. For TM wave in Fig.6(b), the broadband absorption can be maintained to 45° with the absorptivity beyond 80%. When the incident angle increases to 60°, within the broadband width, the absorber still has a good absorptivity greater than 70%. The main reason is that the magnetic flux remains unchanged when the incident angle increases, thus the magnetic resonance in the absorber can be effectively induced. Additionally, the relationship between the absorption and the incident angles at 0.91THz, 1.374THz and 1.772THz is presented in Fig.6(c). At 1.374THz, the good absorptivity beyond 80% remains to 50°, and at 0.91THz and 1.772THz, the absorber remains a good absorptivity beyond 80% to 70°. In conclusion, the proposed absorber can achieve wide angle absorption.

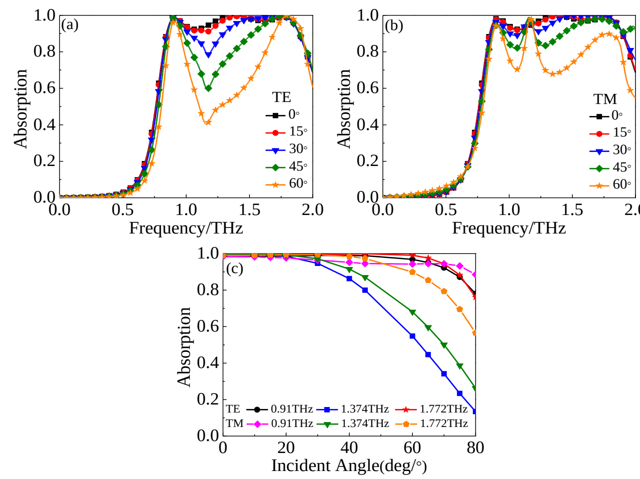

Fig.6. Absorption of the absorber at different incident angles for (a)TE and (b)TM waves and (c)the absorption change at the three peak frequencies with increasing incident angle for both TE and TM waves

Furthermore, the influences of some geometric parameters on the absorption mechanism are discussed. Firstly, the dependence of the absorption on radius change of the outer and inner ring of the metamaterial absorber is studied and depicted in Fig.7. As it is shown in Fig.7, with the radii of the outer and inner ring increasing, red-shift appears at the lower and higher frequency, respectively. It can be concluded that the outer ring mainly account for the lower frequency resonance and the inner ring mainly account for the higher frequency resonance. The results show a great agreement with the surface current distributions that we discussed above. And we can also use the LC circuit model to explain the influence of the radius and the resonant frequency is given by[26]

$$f = \frac{1}{2\pi\sqrt{LC/2}} \propto \frac{1}{l} \tag{1}$$

where l is the diameter of the metallic circular ring. From the equation, it is obvious that the resonant frequency is inversely proportional to the diameter of the circular ring. When the radius increases, the resonances move to lower frequencies accordingly.

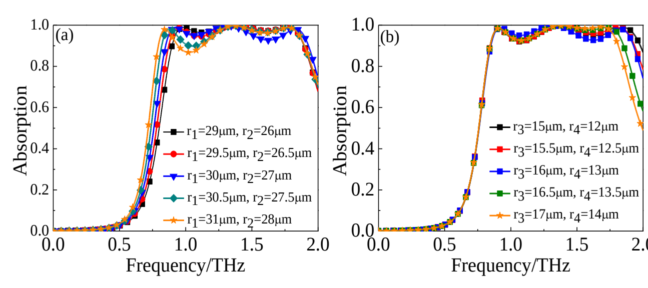

Fig.7. Dependence of the absorption spectra on radius change of the (a) outer ring and (b) inner ring.

This article has been accepted for publication in a future issue of this journal, but has not been fully edited. Content may change prior to final publication. Citation information: DOI 10.1109/JQE.2016.2643279, IEEE Journal of Quantum Electronics

In order to investigate the influence of the thickness of dielectric substrate, the absorption curve is simulated when the thickness t is set to be 26μm, 26.5μm, 27μm, 27.5μm and 28μm, respectively. The simulation result is depicted in Fig.8, which shows a small change in the absorptivity and the absorption band width. And it also can be observed that a slight red-shift occurs at the central frequency. This can be explained by the propagation phase which is given by[35]

$$\varphi_p = \frac{4t\sqrt{\varepsilon_r - \sin^2\theta}}{\lambda} \qquad (2)$$

where φ_p is the propagation phase, t is the thickness of the dielectric layer, ε_r is the real part of permittivity, θ is the incident angle and λ is the terahertz wavelength. Because ε_r=3, θ=0° are fixed values and φ_p is also considered to be a fixed value for the incident wave is plane wave, the value of t/λ is fixed. It means t is proportional to λ and is inversely proportional to the resonant frequency f. So, with the thickness of the dielectric substrate increasing, the central frequency is red shift.

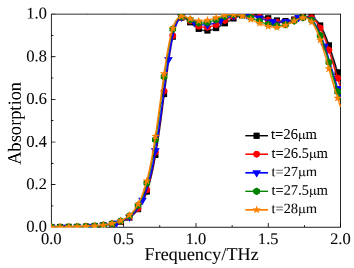

Fig.8. Influence of the thickness of dielectric substrate on absorption

Although, the aforementioned absorber is the circular split-ring shape, the design idea can also be applied to other type structures. For example, it works well for the square split-ring structure shown in Fig.9(a). The parameters of the unit cell are as follows: P=P_x=P_y=70μm, l_1=28μm, l_2=24μm, l_3=17μm, l_4=13μm, w_1=w_2=4μm, and the thickness of the dielectric substrate t is set to 26μm and the material is polyimide with effective electric permittivity ε_r=3 and tangential loss tanσ=0.06. The metal is Au with a thickness of 0.4μm and conductivity of 4.56×10^7S/m. Fig.9(b) shows the simulated absorption curve. It is obvious that the square split-ring absorber achieves a broadband absorption of 0.834THz from 0.77THz to 1.604THz with the absorptivity beyond 90%, and the FWHM (Full Width at Half Maximum) is 105% (with respect to the central frequency). By adjusting the dimensions of the circular split-ring absorber, the absorption can be realized in the microwave regime. The unit cell of the adjusted absorber is shown in Fig.9(c) and the parameters are as follows: P=P_x=P_y=10mm, r_1=4.3mm, r_2=3.9mm, r_3=3mm, r_4=2.6mm, w_1=w_2=0.4mm. The dielectric layer is FR-4 of 3.8mm with effective electric permittivity ε_r=4.3 and tangential loss tanσ=0.025, the material of the metallic layers is copper with a thickness of 0.035mm and conductivity of 5.8×10^7S/m. Figure8(d) shows the simulated absorption curve in microwave range. As shown in Fig.9(d), the presented absorber has a broadband absorption of 4.23GHz from 5GHz to 9.23GHz with the absorptivity greater than 90%, and the FWHM is 4.98GHz which is 71.14% with respect to the central frequency.

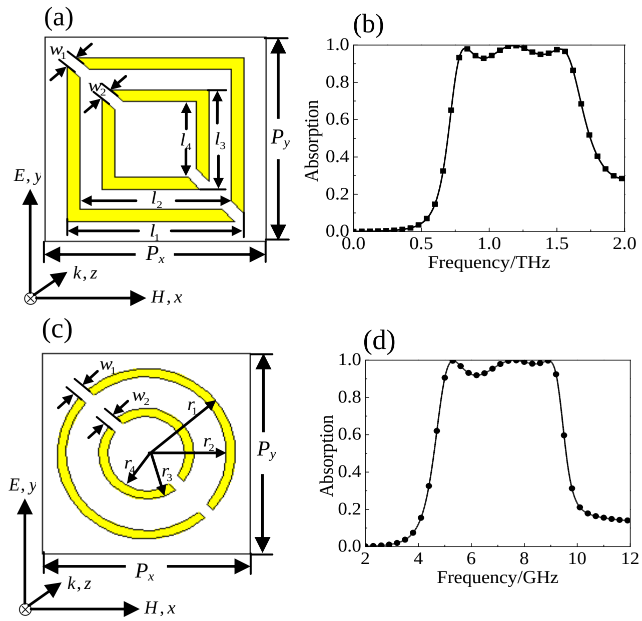

Fig.9. The unit cell of the terahertz absorber(a) and the microwave absorber(c). Simulated absorption curves for the proposed terahertz(b) and microwave (d) absorbers

IV. CONCLUSIONS

In conclusion, we have presented a broadband terahertz metamaterial absorber which is composed of two circular split rings and a grounded metallic film separated by a dielectric substrate. Simulation results show that the absorber achieved a broadband absorption greater than 90% from 0.85THz to 1.926THz for both TE and TM waves, and the width is 1.076THz. The absorption mechanism is illustrated by investigating the surface current distributions and energy density of electromagnetic field. It is found that the high absorptivity is mainly due to strong electromagnetic resonance in the absorber structure. We also studied the influences of incident angles and some geometric parameters on the performance of the metamaterial absorber. The geometry parameters and absorption bandwidth of the proposed absorber has been compared with some other absorbers listed in Table 2. It is found that the bandwidth with absorptivity above 90% of the proposed absorber has been increased greatly as compared to [11] [12] [22] [26]. The idea of the proposed design is not limited to circular split ring absorber, it can also be applied to some other type like the square split ring structure. And by changing the dimensions of the absorber structure, a broadband absorber can be easily realized in the microwave range. Therefore, it provides us a flexible and feasible approach to choose the structure type and the working frequency range of the metamaterial absorber. The proposed broadband metamaterial absorber has many potential applications in terahertz spectrum imaging, detecting and stealthy technology.

Table 2 Comparison of the proposed structure with a few reported broadband absorber structures

Absorber	Centre frequency (THz)	Unit cell size (μm)	Thickness (μm)	Bandwidth with absorptivity above 90%(with respect to centre freqency)
Wang et al.[11]	1.96	85	10.0(0.067λ_0)	15.30%
Wen et al.[12]	4.79	20	3.4(0.056λ_0)	17.12%
Cheng et al.[22]	6.64	38	0.7(0.015λ_0)	12.05%
Huang et al.[26]	0.90	78	8.5(0.025λ_0)	11.11%
Proposed structure	1.388	70	26.0(0.087λ_0)	77.52%

REFERENCES

[1] D. R. Smith, W. J. Padilla, D. Vier, S. C. Nemat-Nasser, and S. Schultz, "Composite medium with simultaneously negative permeability and permittivity," *Phys. Rev. Lett*, vol. 84, no. 18, pp. 4184, 2000..

[2] D. Schurig, J. Mock, B. Justice, S. A. Cummer, J. B. Pendry, A. Starr, and D. Smith, "Metamaterial electromagnetic cloak at microwave frequencies," *Science*, vol. 314, no. 5801, pp. 977-980, 2006.

[3] D. R. Smith, J. B. Pendry, and M. C. Wiltshire, "Metamaterials and negative refractive index," *Science*, vol. 305, no. 5685, pp. 788-792, 2004.

[4] G. Wang, M. Liu, X. Hu, L. Kong, L. Cheng, and Z. Chen, "Broadband and ultra-thin terahertz metamaterial absorber based on multi-circular patches," *Eur Phys J B*, vol. 86, no. 7, pp. 1-9, 2013.

[5] H.-T. Chen, W. J. Padilla, J. M. Zide, A. C. Gossard, A. J. Taylor, and R. D. Averitt, "Active terahertz metamaterial devices," *Nature*, vol. 444, no. 7119, pp. 597-600, 2006.

[6] T. Driscoll, G. Andreev, D. Basov, S. Palit, S. Cho, N. Jokerst, and D. Smith, "Tuned permeability in terahertz split-ring resonators for devices and sensors," *Appl. Phys. Lett*, vol. 91, no. 6, pp. 062511, 2007.

[7] O. Paul, C. Imhof, B. Lńgel, S. Wolff, J. Heinrich, A. Forchel, R. Zengerle, R. Beigang, and M. Rahm, "Polarization-independent active metamaterial for high-frequency terahertz modulation," *Opt. Exp*, vol. 17, no. 2, pp. 819-827, 2009.

[8] N. Landy, S. Sajuyigbe, J. Mock, D. Smith, and W. Padilla, "Perfect metamaterial absorber," *Phys. Rev. Lett*, vol. 100, no. 20, pp. 207402, 2008.

[9] J. Chen, X. Huang, G. Zerihun, Z. Hu, S. Wang, G. Wang, X. Hu, and M. Liu, "Polarization-independent, thin, broadband metamaterial absorber using double-circle rings loaded with lumped resistances," *J. Electron. Mater*, vol. 44, no. 11, pp. 4269-4274, 2015.

[10] S. Bhattacharyya, S. Ghosh, D. Chaurasiya, and K. V. Srivastava, "Wide-angle broadband microwave metamaterial absorber with octave bandwidth," *IET Microw Antenna P*, vol. 9, no. 11, pp. 1160-1166, 2015.

[11] B.-X. Wang, L.-L. Wang, G.-Z. Wang, W.-Q. Huang, X.-F. Li, and X. Zhai, "Theoretical investigation of broadband and wide-angle terahertz metamaterial absorber," *IEEE Photon Technol Lett*, vol. 26, no. 2, pp. 111-114, 2014.

[12] Y. Wen, W. Ma, J. Bailey, G. Matmon, and X. Yu, "Broadband terahertz metamaterial absorber based on asymmetric resonators with perfect absorption," *IEEE T Thz Sci Techn*, vol. 5, no. 3, pp. 406-411, 2015.

[13] J. A. Mason, G. Allen, V. A. Podolskiy, and D. Wasserman, "Strong coupling of molecular and mid-infrared perfect absorber resonances," *IEEE Photon Technol Lett*, vol. 24, no. 1, pp. 31-33, 2012.

[14] M. K. Hedayati, M. Javaherirahim, B. Mozooni, R. Abdelaziz, A. Tavassolizadeh, V. S. K. Chakravadhanula, V. Zaporojtchenko, T. Strunkus, F. Faupel, and M. Elbahri, "Design of a perfect black absorber at visible frequencies using plasmonic metamaterials," *Adv Mater*, vol. 23, no. 45, pp. 5410-5414, 2011.

[15] Q.-Y. Wen, H.-W. Zhang, Y.-S. Xie, Q.-H. Yang, and Y.-L. Liu, "Dual band terahertz metamaterial absorber: Design, fabrication, and characterization," *Appl Phys Lett*, vol. 95, no. 24, pp. 241111, 2009.

[16] H. Tao, C. Bingham, D. Pilon, K. Fan, A. Strikwerda, D. Shrekenhamer, W. Padilla, X. Zhang, and R. Averitt, "A dual band terahertz metamaterial absorber," *J Phys D Appl Phys*, vol. 43, no. 22, pp. 225102, 2010.

[17] M. Li, H.-L. Yang, X.-W. Hou, Y. Tian, and D.-Y. Hou, "Perfect metamaterial absorber with dual bands," *Prog Electromagn Res*, vol. 108, pp. 37-49, 2010.

[18] H.-X. Xu, G.-M. Wang, M.-Q. Qi, J.-G. Liang, J.-Q. Gong, and Z.-M. Xu, "Triple-band polarization-insensitive wide-angle ultra-miniature metamaterial transmission line absorber," *Phys Rev B*, vol. 86, no. 20, pp. 205104, 2012.

[19] L. Huang, and H. Chen, "Multi-band and polarization insensitive metamaterial absorber," *Prog Electromagn Res*, vol. 113, pp. 103-110, 2011.

[20] B.-X. Wang, X. Zhai, G. Wang, W. Huang, and L. Wang, "Design of a four-band and polarization-insensitive terahertz metamaterial absorber," *IEEE Photon J*, vol. 7, no. 1, pp. 1-8, 2015.

[21] S. He, and T. Chen, "Broadband THz absorbers with graphene-based anisotropic metamaterial films," *IEEE T Thz Sci Technol*, vol. 3, no. 6, pp. 757-763, 2013.

[22] Y. Cheng, Y. Nie, and R. Gong, "A polarization-insensitive and omnidirectional broadband terahertz metamaterial absorber based on coplanar multi-squares films," *Opt Laser Technol*, vol. 48, pp. 415-421, 2013.

[23] H. Xiong, J.-S. Hong, C.-M. Luo, and L.-L. Zhong, "An ultrathin and broadband metamaterial absorber using multi-layer structures," *J Appl Phys*, vol. 114, no. 6, pp. 064109, 2013.

[24] J. Grant, Y. Ma, S. Saha, A. Khalid, and D. R. Cumming, "Polarization insensitive, broadband terahertz metamaterial absorber," *Opt Lett*, vol. 36, no. 17, pp. 3476-3478, 2011.

[25] Y. Q. Ye, Y. Jin, and S. He, "Omnidirectional, polarization-insensitive and broadband thin absorber in the terahertz regime," *J Opt Soc Am B*, vol. 27, no. 3, pp. 498-504, 2010.

[26] L. Huang, D. R. Chowdhury, S. Ramani, M. T. Reiten, S.-N. Luo, A. J. Taylor, and H.-T. Chen, "Experimental demonstration of terahertz metamaterial absorbers with a broad and flat high absorption band," *Opt Lett*, vol. 37, no. 2, pp. 154-156, 2012.

[27] S. Bhattacharyya. "A Broadband Microwave Metamaterial Absorber with Octave Bandwidth," *Mapan*, vol. 31, no. 4, pp. 299-307, 2016.

[28] S. Bhattacharyya, S. Ghosh, K. V. Srivastva. "A microwave metamaterial absorber with wide bandwidth," presented at *IEEE URSI AP-RASC*, pp.1215-1218, 2016.

[29] B.-X. Wang, G.-Z. Wang, and L.-L. Wang, "Design of a novel dual-band terahertz metamaterial absorber," *Plasmonics*, vol. 11, no. 2, pp. 523-530, 2016.

[30] Y. J. Kim, Y. J. Yoo, K. W. Kim, J. Y. Rhee, Y. H. Kim, and Y. Lee, "Dual broadband metamaterial absorber," *Opt. Exp*., vol. 23, no. 4, pp. 3861-3868, 2015.

[31] X. Liu, T. Starr, A. F. Starr, and W. J. Padilla, "Infrared spatial and frequency selective metamaterial with near-unity absorbance," *Phys. Rev. Lett*, vol. 104, no. 20, pp. 207403, 2010.

[32] J.-F. Wang, S.-B. Qu, Z. Xu, Y.-M. Yang, C. Gu. "A controllable magnetic metamaterial: split-ring resonator with rotated inner ring," *IEEE T Antenn Propag*, vol. 56, no. 7, pp. 2018-2022, 2008.

[33] J.-F. Zhou, T. Koschny, M. Kafesaki, C. M. Soukoulis. "Size dependence and convergence of the retrieval parameters of metamaterials," *Photonic Nanostruct*., vol. 6, no. 1, pp. 96-101, 2008.

[34] K. B. Alici, and E. Ozbay, "A planar metamaterial: Polarization independent fishnet structure," *Photonic Nanostruct*, vol. 6, no. 1, pp. 102-107, 2008.

[35] T.-B. Zou, F.-R. Hu, J. Xiao, L.-H. Zhang, F. Liu, Chen Tao, J.-H. Niu, X.-M. Xiong, "Design of a polarization-insensitive and broadband terahertz absorber using metamaterials," *Acta. Phys. Sin-CH. ED*., vol. 63, no. 17, p. 178103, Sep. 2014.

Wu Pan: received the Ph.D Degree in Precision Instrument and Machinery from the School of Photoelectronic Engineering, Chongqing University, Chongqing, China, in June 2001.
He is currently a professor at the School of Optical and Electrical Engineering, Chongqing University of Posts and Telecommunications, Chongqing, China. His research interests include Terahertz technology, metamaterials devices and their applications.

Xuan Yu: received the B.S. degree in Optical Information Science and Technology from the School of Photoelectronic Engineering, Chongqing University of Posts and Telecommunications, Chongqing, China, in June 2014.
She is currently pursuing the M.S. Degree in Optical Engineering, her research interests include metamaterials and their applications, in particular the perfect absorption in Terahertz radiation.

Jun Zhang: received the B.S. degree in Optical Information Science and Technology from the School of Photoelectronic Engineering, Chongqing University of Posts and Telecommunications, Chongqing, China, in June 2014.
She is currently pursuing the M.S. Degree in Integrated Circuit Engineering, her research interests include metamaterials and their applications, in particular the metamaterial filter in Terahertz radiation.

Wei Zeng: received the B.S. degree in Optical Information Science and Technology from the School of Photoelectronic Engineering, Chongqing University of Posts and Telecommunications, Chongqing, China, in June 2014.
He is currently pursuing the M.S. Degree in Optical Engineering, his research interests include Terahertz technology and its application, in particular the Terahertz communication lens antenna.